Cytochrome P450 and Aromatic Bases: A ^{1}H NMR Study

Lucia Banci,† Ivano Bertini,*,† Simonetta Marconi,† Roberta Pierattelli,† and Stephen G. Sligar‡

Contribution from the Department of Chemistry, University of Florence, Via G. Capponi 7, 50121 Florence, Italy, and Department of Biochemistry and Chemistry, The University of Illinois, 600 South Matthews Avenue, Urbana, Illinois 61801

Received October 4, 1993®

Abstract: Camphor-free cytochrome P450 (Cyt P450) from *Pseudomonas putida* has been investigated in the presence of aromatic bases like pyridine, imidazole, and *N*-methylimidazole. ^{1}H NMR signals of the heme protons indicate that the bases bind both in the hydrophobic cavity and at the metal. Even a ternary Cyt P450–pyridine–imidazole system has been detected. The electronic spectra are capable of monitoring the binding at the metal. The derivatives with these bases are low spin and their ^{1}H NMR spectra have been investigated through DNOE and 2D NOESY spectroscopy. An assignment of some heme protons is proposed. This represents the first high-resolution NMR study on Cyt P450. Through saturation-transfer spectroscopy a partial assignment has been made on the high-spin Cyt $P450_{cam}$.

Introduction

Cytochromes P450 (P450 hereafter) are a ubiquitous class of heme proteins that catalyze the hydroxylation of a large variety of aliphatic and aromatic compounds.[1] Among these enzymes, cytochrome $P450_{cam}$, obtained by growing *Pseudomonas putida* on *d*-camphor,[2,3] is the most studied due to its solubility, relative stability, and ease of purification. It catalyzes the oxygen insertion into the camphor molecule.[4]

$P450_{cam}$ is a single polypeptide chain (MW 45 000) with a protoheme IX as prosthetic group. The crystal structure of the camphor-bound and camphor-free enzyme has been obtained at high resolution,[5,6] confirming that a cysteine is the fifth axial ligand, as previously suggested on the basis of EPR studies.[7-10]

The substrate-free form (P450) has a solvent molecule in the sixth coordination position. This was found in the X-ray structure,[6] and it was earlier proposed on the basis of water proton NMR relaxation measurements.[11,12] On the basis of the analysis of several adduct structures, of the patterns of the redox potential values,[13] and of the spin states, it has been proposed that the iron-bound solvent molecule is in the OH form.[14,15] In the presence of the natural substrate, camphor, the iron(III) ion is pentacoordinated and is in the high-spin state, due to the displacement of the solvent molecule by the substrate molecule.[5,6,16,17]

The existence of spin equilibrium between the solvent-free high-spin and the solvent-bound low-spin iron has been found in P450 isolated from different sources.[18,19] EPR has been widely applied to study the spin states at low temperature.[20,21] For studies at physiological conditions, other physical methods have been used, such as UV–vis spectroscopy, CD, and MCD.[21] Earlier studies on the interactions of various ligands with the active center of $P450_{cam}$ were mainly focused on the identification of the axial ligands. Once the nature of the iron(III) ion ligands is established, it is important to elucidate the electronic structure and the ligand coordination properties. P450 inhibitors are usually classified according to the modification that they produce on the maximum absorption of the Soret band. Most compounds oxidized by P450 produce a blue shift of the maximum of the Soret absorption, stabilizing the high-spin form, whereas compounds having donor groups capable of binding to the metal move the Soret absorption to the red region, shifting the spin equilibrium to low spin.[22]

X-ray structures have been reported for large numbers of adducts with non-natural substrates, for which different binding modes have been observed.[14-16,23] The size of the ligand molecule and its ability to interact with protein residues determine the affinity. The nature, the size, and the steric crowding of the ligand determine also the displacement or the presence of the axial solvent ligand and its protonation state.[16] The latter properties have been proposed to determine the spin state (low or high spin) of the iron(III) in the adducts.[16]

NMR spectroscopy has not been applied as extensively as other spectroscopic techniques to P450. This is mainly due to the low spectral resolution of the spectrum of this protein, especially in the low-spin form, which is characterized by small hyperfine shift values and large line widths.[24-27] For the study of ligand binding

† University of Florence.
‡ The University of Illinois.
* Abstract published in *Advance ACS Abstracts,* May 1, 1994.

(1) Wislocki, P. G.; Miwa, G. T.; Lu, A. Y. In *Enzymatic basis of detoxification*; Jacoby, W. B., Ed., Academic Press: New York, 1980; pp 135–182.
(2) Hedegaard, J.; Gunsalus, I. C. *J. Biol. Chem.* **1965**, *240*, 4038.
(3) Gunsalus, I. C.; Sligar, S. G. *Adv. Enzymol. Relat. Areas Mol. Biol.* **1978**, *47*, 1.
(4) Katagiri, M.; Ganguli, B. N.; Gunsalus, I. C. *J. Biol. Chem.* **1968**, *243*, 3543.
(5) Poulos, T. L.; Finzel, B. C.; Howard, A. J. *J. Mol. Biol.* **1987**, *195*, 687.
(6) Poulos, T. L.; Finzel, B. C.; Howard, A. J. *Biochemistry* **1986**, *25*, 5314.
(7) Collman, J. P.; Sorrell, Th. N.; Hoffmann, B. M. *J. Am. Chem. Soc.* **1975**, *97*, 913.
(8) Koch, S.; Tang, S. C.; Holm, R. H.; Frankel, R. B.; Ibers, J. A. *J. Am. Chem. Soc.* **1975**, *97*, 917.
(9) Tang, S. C.; Koch, S.; Papaefthyomyou, G. C.; Foner, S.; Frankel, R. B.; Ibers, J. A.; Holm, R. H. *J. Am. Chem. Soc.* **1976**, *98*, 2414.
(10) Collman, J. P.; Sorrell, Th. N.; Hodgson, K. O.; Kulshrestha, A. K.; Strouse, C. E. *J. Am. Chem. Soc.* **1977**, *99*, 5180.
(11) Griffin, B. W.; Peterson, J. A. *J. Biol. Chem.* **1975**, *250*, 6445.
(12) Philson, S. B.; Debrunner, P. G.; Schmidt, P. G.; Gunsalus, I. C. *J. Biol. Chem.* **1979**, *254*, 10173.
(13) Sligar, S. G.; Gunsalus, I. C. *Proc. Natl. Acad. Sci. U.S.A.* **1976**, *73*, 1078.
(14) Raag, R.; Poulos, T. L. *Biochemistry* **1991**, *30*, 2674.
(15) Poulos, T. L.; Howard, A. J. *Biochemistry* **1987**, *26*, 8165.
(16) Raag, R.; Poulos, T. L. *Biochemistry* **1989**, *28*, 917.
(17) Fisher, M. T.; Sligar, S. G. *Biochemistry* **1987**, *26*, 4797.
(18) Whysner, J. A.; Ramseyer, J.; Harding, B. W. *J. Biol. Chem.* **1970**, *245*, 5441.
(19) Bell, J. J.; Cheng, S. C.; Harding, B. W. *Ann. N.Y. Acad. Sci.* **1973**, *212*, 290.
(20) Weiner, L. M. *CRC Crit. Rev. Biochem.* **1986**, *20*, 139.
(21) Dawson, J. H.; Sono, M. *Chem. Rev.* **1987**, *87*, 1255.
(22) Dawson, J. H.; Andersson, L. A.; Sono, M. *J. Biol. Chem.* **1982**, *257*, 3606.
(23) Raag, R.; Swanson, B. A.; Poulos, T. L.; Ortiz de Montellano, P. R. *Biochemistry* **1990**, *29*, 8119.
(24) Lukat, G. S.; Goff, H. M. *Biochim. Biophys. Acta* **1990**, *1037*, 351.
(25) Keller, R. M.; Wüthrich, K. J.; Debrunner, P. G. *Proc. Natl. Acad. Sci. U.S.A.* **1972**, *69*, 2073.

0002-7863/94/1516-4866$04.50/0

to P450, NMR was mostly used to characterize the paramagnetic effects on the proton ligand signals, due to the interaction with the heme moiety.[20]

High-resolution NMR of paramagnetic molecules, when applicable, allows a detailed characterization of the residues around the metal ion.[28-31] Furthermore, it could provide information about the binding mode of substrates and inhibitors. With this in mind, we have undertaken an NMR study of $P450_{cam}$–aromatic base adducts, which have been characterized through EPR and electronic spectroscopy.[22,32,33] Through NMR we have discovered a complex behavior. The knowledge of the properties of these systems is relevant with respect to the comprehension of the protein residues–inhibitor interaction which is responsible for the binding of substrates in the active cavity. We have therefore selected the most favorable system for extensive NMR studies.

Materials and Methods

Cytochrome $P450_{cam}$ was overproduced in *Escherichia coli* strain TB1. This protein was purified by the method of Gunsalus and Wagner[34] with some modifications.[35] Purified $P450_{cam}$ with $A_{391}/A_{280} \approx 1.45$ was concentrated to 0.5 mM in 50 mM potassium phosphate, 1 mM camphor, 20 mM β-ME, 50 mM KCl, pH 7.1, and stored in liquid nitrogen.

Camphor was removed from $P450_{cam}$ by chromatography on a Sephadex G-10 column (1 × 10 cm) equilibrated with 50 mM Tris–HCl (pH 7.4), and the free enzyme solution was then made 50 mM in KCl.

P450 ligand complexes were prepared by titration of the camphor-free protein in 50 mM Tris–HCl, 50 mM KCl (pH 7.4), until no changes were observed in the ^{1}H NMR spectra. The ligands were dissolved in the buffer solution.

Electronic spectra were recorded on a Cary 3 spectrometer at 295 K. The samples were (1.0–2.0) × 10^{-5} M, 50 mM Tris–HCl (pH 7.4), 50 mM KCl, in H_2O.

^{1}H NMR spectra were recorded at 295 and 301 K on a Bruker MSL 200 and on a Bruker AMX 600 operating at 200.13 and 600.14 MHz, respectively. The samples were 0.5–1.0 mM in 50 mM Tris–HCl, 50 mM KCl (pH 7.4), in H_2O or 50 mM phosphate buffer (pH 7.1) and 50 mM KCl in D_2O solution. ^{1}H NMR spectra were performed with the SuperWEFT[36] pulse sequence, using various recycle times, or by presaturating the solvent signal during the relaxation delay. Signal intensity was determined using either the integration routine or the signal deconvolution algorithms of the Bruker UXNMR software package. T_1 measurements were obtained by using the inversion recovery method.[37] The data were fitted by a nonlinear best fitting procedure, using the proper equations. The ^{1}H NOE experiments were performed with the SuperWEFT pulse sequence for water signal suppression and were collected using previous reported methodology.[38,39] Saturation-transfer experiments were performed on samples containing two different species. The exchange rates are calculated according to the following equation:[40]

$$\tau_A = T_1^A \frac{M_Z^A/M_0^A - M_Z^A/M_0^B}{1 - M_Z^A/M_0^A}$$

where A denotes the species on whose signals we observe saturation transfer effect, B is the species whose signals are irradiated, M_Z and M_0 are the magnetizations observed with and without irradiation of the B signal, respectively, and T_1^A is the longitudinal relaxation time of the nucleus in the A environment in the absence of exchange (i.e. pure A species).

The obtainment of selective saturation and artifact-free difference spectra in NOE and saturation-transfer experiments required special experimental care. Difference spectra were collected directly, by applying the decoupler frequency on- and off-resonance, alternatively, according to the scheme ω, $\omega + \delta$, ω, $\omega - \delta$. ω is the frequency of the irradiated signal, and δ is the offset for the off-resonance irradiation. The application of the off-resonance decoupling on both sides of the saturated signal minimized the off-resonance effects in the saturation. The phase of the receiver was alternated accordingly, so that a difference free induction decay was directly collected. In some cases of saturation-transfer effects on signals close to the saturated one, the results were counterchecked by other experiments in which the off-resonance frequency was placed on the other side of the responding signal, symmetrically with respect to the saturated one. NOESY experiments[41] were recorded with presaturation of the solvent signal during both the relaxation delay (150–450 ms) and the mixing time (10–50 ms). The data were collected using the TPPI method.[42] Arrays of 512 FIDs of 1024 data points were acquired. Zero filling in the F1 dimension was applied to obtain a 1024 × 1024 data point matrix. Sine-bell-squared weighting functions with 45–60° phase shifts were applied to the data. An NOE–NOESY experiment[43] with a mixing time of 20 ms was performed by using the conventional NOESY sequence, preceded by a selective irradiation (400 ms) of signal B of the pyridine adduct.

Structure inspection and search for protons within a sphere centered on a given proton were performed with the routines included in the SYBYL program from Tripos Associates Inc.

Results

Figure 1 shows the ^{1}H NMR spectrum of P450 in the presence of camphor. It is in complete agreement with the spectra already reported.[24,27] The large spreading of the paramagnetic shifted signals and their short T_1 and large line widths (see Table 1) are consistent with the $S = {}^5/_2$ nature of iron(III).[28,44] Curie relaxation contributions to the line widths, which depend on the square of the external magnetic field and on the spin multiplicity as well as on the rotational correlation time,[45] are sizable, as also observed in the case of high-spin peroxidases,[31,46] which are also heme proteins with large molecular weight. Indeed, the line widths are smaller at 200 MHz than at 600 MHz (see Table 1). The pseudocontact shift contributions are small, again consistent with the $S = {}^5/_2$ nature of the systems,[47] thus limiting the resolution outside the diamagnetic envelope only to those protons which belong to metal ion ligands.

On the contrary, low-spin iron(III)-containing species are generally characterized by narrow line widths and large pseudocontact shift contributions, which increase the number of signals outside the diamagnetic envelope even if they are spread over a small spectral range.[31,46]

The ^{1}H NMR spectrum of the low-spin species obtained in the absence of camphor is reported in Figure 2a. The two most downfield-shifted signals in the spectrum have a relative intensity of 3 and shift values consistent with those already reported for

(26) Sato, R.; Omura, T. *Cytochrome P450*; Academic Press: New York, 1978.
(27) Banci, L.; Bertini, I.; Eltis, L. D.; Pierattelli, R. *Biophys. J.* **1993**, *65*, 806.
(28) Johnson, M. E.; Fung, L. W.-M.; Ho, C. *J. Am. Chem. Soc.* **1977**, *99*, 1245.
(29) Satterlee, J. D. In *Metal ions in biological systems*; Sigel, H., Ed.; Marcel Dekker: New York, 1987; pp 121–185.
(30) La Mar, G. N. In *Biological Applications of Magnetic Resonance*; Shulman, R. G., Ed.; Academic: New York, 1979; pp 305–343.
(31) Bertini, I.; Turano, P.; Vila, A. J. *Chem. Rev.* **1993**, *93*, 2833.
(32) Lipscomb, J. D. *Biochemistry* **1980**, *19*, 3590.
(33) Ruf, H. H.; Wende, P.; Ullrich, V. *J. Inorg. Biochem.* **1979**, *11*, 189.
(34) Gunsalus, I. C.; Wagner, G. C. *Methods Enzymol.* **1978**, *52*, 166.
(35) Unger, B. P.; Gunsalus, I. C.; Sligar, S. G. *J. Biol. Chem.* **1986**, *261*, 1158.
(36) Inubushi, T.; Becker, E. D. *J. Magn. Reson.* **1983**, *51*, 128.
(37) Vold, R. L.; Waugh, J. S.; Klein, M. P.; Phelps, D. E. *J. Chem. Phys.* **1968**, *48*, 3831.
(38) Thanabal, V.; de Ropp, J. S.; La Mar, G. N. *J. Am. Chem. Soc.* **1987**, *109*, 7516.
(39) Banci, L.; Bertini, I.; Luchinat, C.; Piccioli, M.; Scozzafava, A.; Turano, P. *Inorg. Chem.* **1989**, *28*, 4650.
(40) Gupta, R. K.; Redfield, A. G. *Biochem. Biophys. Res. Commun.* **1970**, *41*, 273.
(41) Macura, S.; Wüthrich, K. J.; Ernst, R. R. *J. Magn. Reson.* **1982**, *47*, 351.
(42) Marion, D.; Wüthrich, K. J. *Biochem. Biophys. Res. Commun.* **1982**, *113*, 967.
(43) Bertini, I.; Dikiy, A.; Luchinat, C.; Piccioli, M.; Tarchi, D. *J. Magn. Reson.*, in press.
(44) La Mar, G. N. In *NMR of Paramagnetic Molecules*; La Mar, G. N., Horrocks, W. D., Jr., Holm, R. H. Eds.; Academic Press: New York, 1973.
(45) Vega, A. J.; Fiat, D. *Mol. Phys.* **1976**, *31*, 347.
(46) Bertini, I.; Luchinat, C. *NMR of Paramagnetic Molecules in Biological Systems*; Benjamin/Cummings: Menlo Park, CA, 1986.
(47) La Mar, G. N.; Walker, F. A. In *The Porphyrins*; Dolphin, D., Ed.; Academic Press: New York, 1979; pp 61–157.

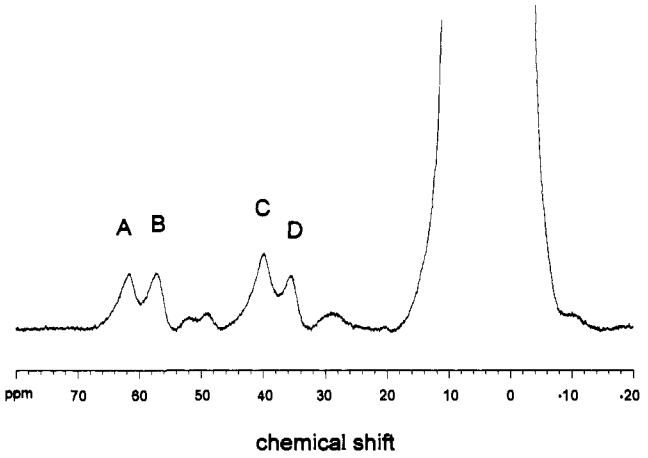

Figure 1. 600-MHz ^{1}H NMR spectrum of P450$_{cam}$ at 295 K. The protein sample was in 50 mM phosphate buffer (pH 7.1), 50 mM KCl, and 1 mM camphor in D_2O solution.

Table 1. Chemical Shift, T_1, and Line Width Values for the Four Methyl Signals of High-Spin P450$_{cam}$

		200 MHz		
P450$_{cam}$ signal	δ, ppm	T_1,[a] ms	$\Delta\nu$, Hz	600 MHz $\Delta\nu$, Hz
A	63.4	3.9	380	2000
B	58.5	4.1	400	1600
C	40.9	5.8	380	2300
D	36.3	5.5	340	1400

[a] T_1 values were measured with an error of ±15%.

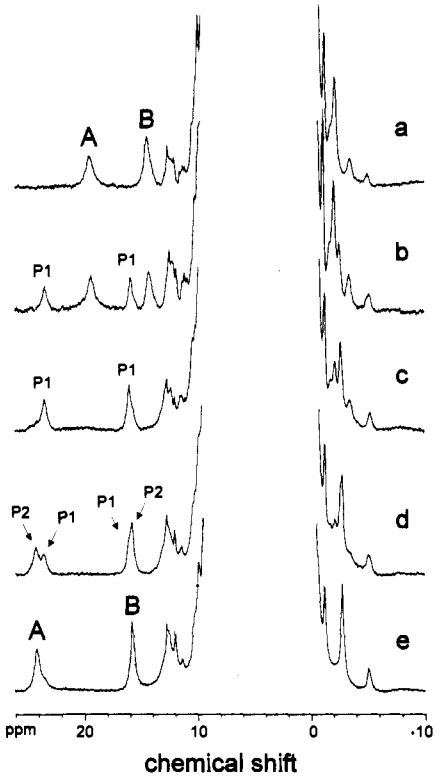

Figure 2. 600-MHz ^{1}H NMR titration of P450 with pyridine, recorded at 600 MHz and 295 K. The sample was 0.7 mM in 50 mM Tris–HCl and 50 mM KCl (pH 7.4) in H_2O: (a) P450; (b) P450 + 0.4 equiv of pyridine; (c) P450 + 1.3 equiv of pyridine; (d) P450 + 5 equiv of pyridine; (e) P450 + 18 equiv of pyridine.

a previous NMR spectrum recorded at 360 MHz.[12] The present spectrum also shows a composite signal centered at about 12.5 ppm and some resolved signals in the upfield part of the spectrum.

Low-spin iron(III) species are produced also by the binding of a sixth ligand to the iron. Among the ligands which provide the low-spin species, we have studied imidazole, *N*-methylimidazole, and pyridine. They had been already characterized through EPR and electronic spectroscopy.[22,32,33] The EPR values (g_1 = 2.46–2.56, g_2 = 2.26–2.27, g_3 = 1.87–1.92) are indicative of relatively low magnetic anisotropies. The g values for P450 are g_1 = 2.45, g_2 = 2.26, and g_3 = 1.91.[22]

Titration of P450 with Pyridine. The effect of pyridine on the ^{1}H NMR spectra of P450 is reported in Figure 2. By addition of increasing amounts of pyridine we observe the formation of a species (P1) which is in slow exchange with the free species and contains low-spin iron(III). The formation is essentially complete with 1.3 equiv of pyridine. The spectrum of P1 is reported in Figure 2c. By further addition of pyridine, another species (P2) is formed which is in slow exchange with species P1. The complete formation of P2 occurs by addition of about 18 equiv of pyridine. Addition of 1 equiv of pyridine and formation of P1 induce variations of about 4 ppm on signal A and of 1.5 ppm on signal B with respect to P450. These changes are larger than those observed upon formation of P2 and P1 (1 and 0.5 ppm, respectively). By measurement of the variation of the NMR signal intensity as a function of pyridine concentration a large affinity constant K ($>10^4$ M^{-1}) for the first adduct can be estimated, while the K for the second equivalent is of the order of 1×10^3 M^{-1}.

The electronic spectra of the pyridine adducts clarify the binding mode of pyridine. The titration is reported in Figure 3. Addition of pyridine affects essentially the Soret band, which is moved from 417 to 421 nm, and the α transition. By fitting with a nonlinear least-squares procedure the variation of intensity at 571 nm, an affinity constant K of $2.2 \times 10^4 \pm 8\%$ M^{-1} is calculated. Similar values are obtained by fitting the absorbance variation at other wavelengths. This value is consistent with the NMR estimate. After the formation of this species, only a small change in the absorbance is observed for higher pyridine concentrations, but no evidence of a second binding constant is detected. This behavior indicates that the electronic spectra monitor the binding of the first equivalent of pyridine, while the binding of the second equivalent produces only minor effects on the Soret band.

The changes in the NMR spectra as well as the behavior along the spectrophotometric titration lead us to propose that the first equivalent of pyridine binds to the iron, while the second equivalent is located in the hydrophobic pocket.

X-ray data have shown that there are two possible binding sites and that ligands, depending essentially on their steric properties, can bind either in the camphor binding site or at the metal.[14–16] Our NMR measurements on relatively small molecules indicate that the protein can bind simultaneously to two ligands.

^{1}H NMR Titration of P450$_{cam}$ with Pyridine. To better characterize the interaction of P450 with pyridine, titration has also been performed on the protein complex with camphor (Figure 4). Upon addition of pyridine, the spectrum of a new species, P1′, is formed. Its spectrum is identical to that of P1. With increasing amounts of pyridine, a second species, P2′, starts to appear, the P1′ species being not yet completely formed and some P450$_{cam}$ being still present. With pyridine in excess, only the spectrum of the second species remains, which is identical to the spectrum of P2. Again, P450$_{cam}$, P1, and P2 are in slow exchange. The presence of camphor changes the relative distribution of P1 and P2, decreasing the affinity of pyridine for P450. The first molecule of pyridine binds to the iron, displacing the camphor molecule from the hydrophobic pocket. The second equivalent begins being bound when the P1 adduct is not fully formed. This suggests that the binding constants of pyridine for P450$_{cam}$ and for P1 have similar values, with the former being slightly larger than the latter.

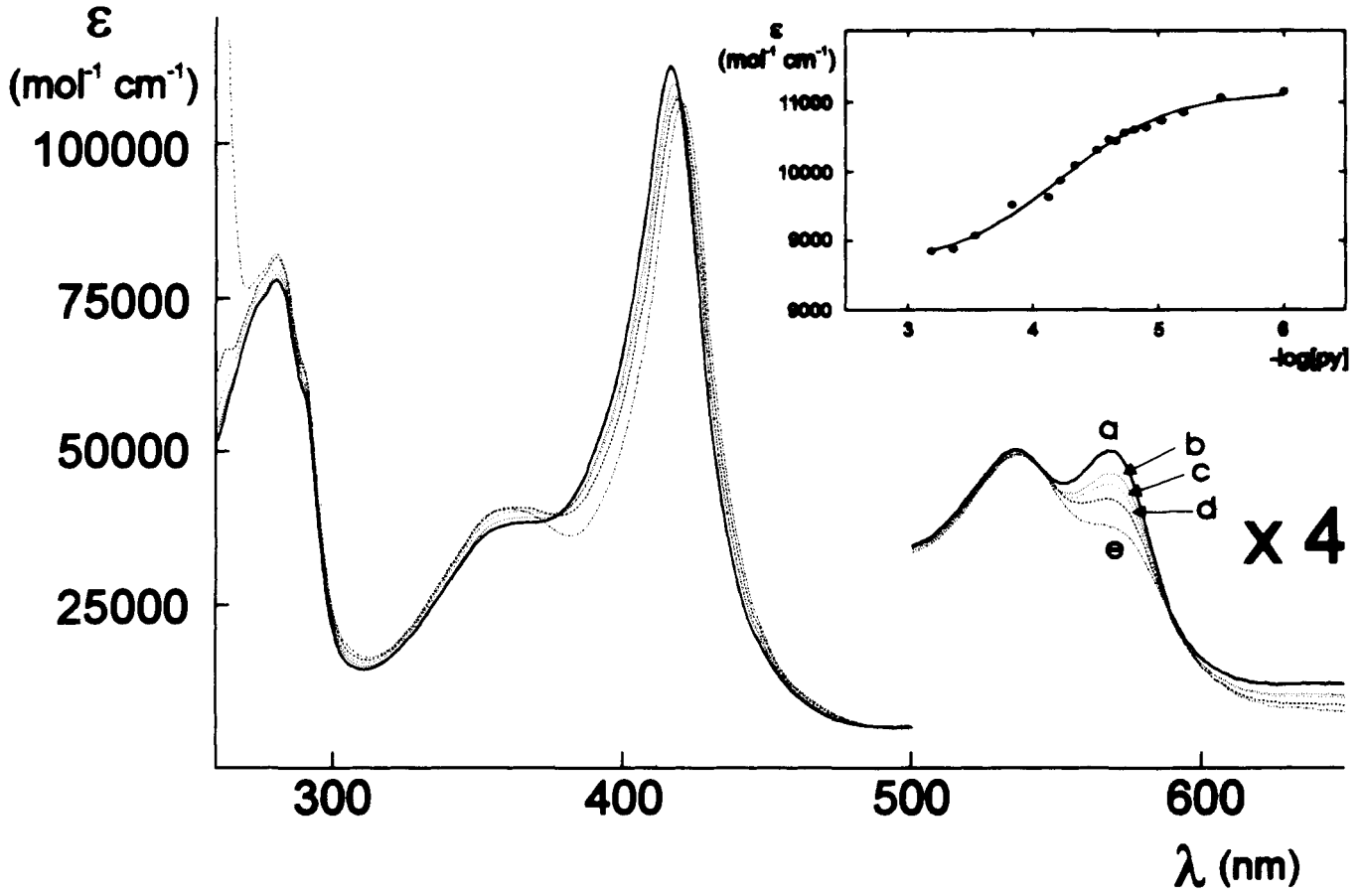

Figure 3. Electronic spectra of the P450 as a function of increasing additions of pyridine. The sample was 1.6×10^{-5} M in 50 mM Tris–HCl and 50 mM KCl (pH 7.4) in H_2O: (a) P450; (b) P450 + 1 equiv of pyridine; (c) P450 + 2 equiv of pyridine; (d) P450 + 5 equiv of pyridine; (e) P450 + 50 equiv of pyridine. The titration curve (at 571 nm) is shown as an inset.

^{1}H NMR Titration of P450 with Imidazole and *N*-Methylimidazole and Further Titration with Pyridine. In order to further characterize the binding of aromatic molecules to P450, we have also performed the titration of P450 with imidazole and *N*-methylimidazole. The interaction of P450 with the two molecules is very similar. They both provide low-spin iron(III)-containing species. They also have two binding sites; however, at variance with pyridine, the distribution of the two species (I1 and I2 for imidazole and N1 and N2 for *N*-methylimidazole) is essentially the same along the titration. The I1 and N1 adducts have very similar NMR spectra. The final I2 and N2 adducts have slightly different shift values for the two resolved heme methyl signals. Also for these ligands, the bound molecules are in slow exchange with the free bases as well as between metal-bound and cavity-bound molecules. Saturation-transfer experiments on a mixture of P450 and I1 do not show any effect, thus indicating that the exchange rate is slower than 10 s^{-1}. On the contrary, transfer of saturation is observed between I1 and I2 (Figure 5) both by saturating a signal of the I1 species and by saturating the corresponding signal in I2. This indicates that the second imidazole molecule is in faster exchange with the bulk one than the first. The exchange rate can be estimated from both saturation-transfer experiments to be around 30 s^{-1}. These experiments were carried out with particular care, as described under Materials and Methods, because the short T_1's of the signals involved make their selective saturation difficult and therefore it is possible that artifacts will arise.

In order to learn which is the metal-bound and which is the cavity-bound species, we have performed a titration with pyridine starting from the imidazole adduct. The affinity constant of pyridine for the imidazole adduct should be smaller than that for P450. We start from a sample which contains the two imidazole adducts, i.e. I1 and I2. By addition of increasing amounts of pyridine, three further species are formed while the I1 and I2 forms are still present. Two species are the two pyridine adducts,

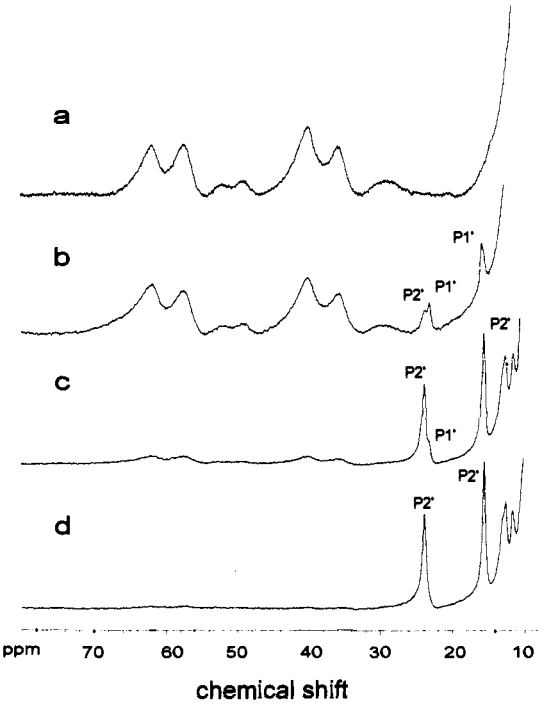

Figure 4. 600-MHz ^{1}H NMR titration of $P450_{cam}$ with pyridine, recorded at 600 MHz and 295 K. The protein concentration was 1 mM in 50 mM phosphate buffer (pH 7.1), 50 mM KCl, and 1 mM camphor in D_2O solution: (a) $P450_{cam}$; (b) P450 + 1 equiv of pyridine; (c) P450 + 10 equiv of pyridine; (d) P450 + 22 equiv of pyridine.

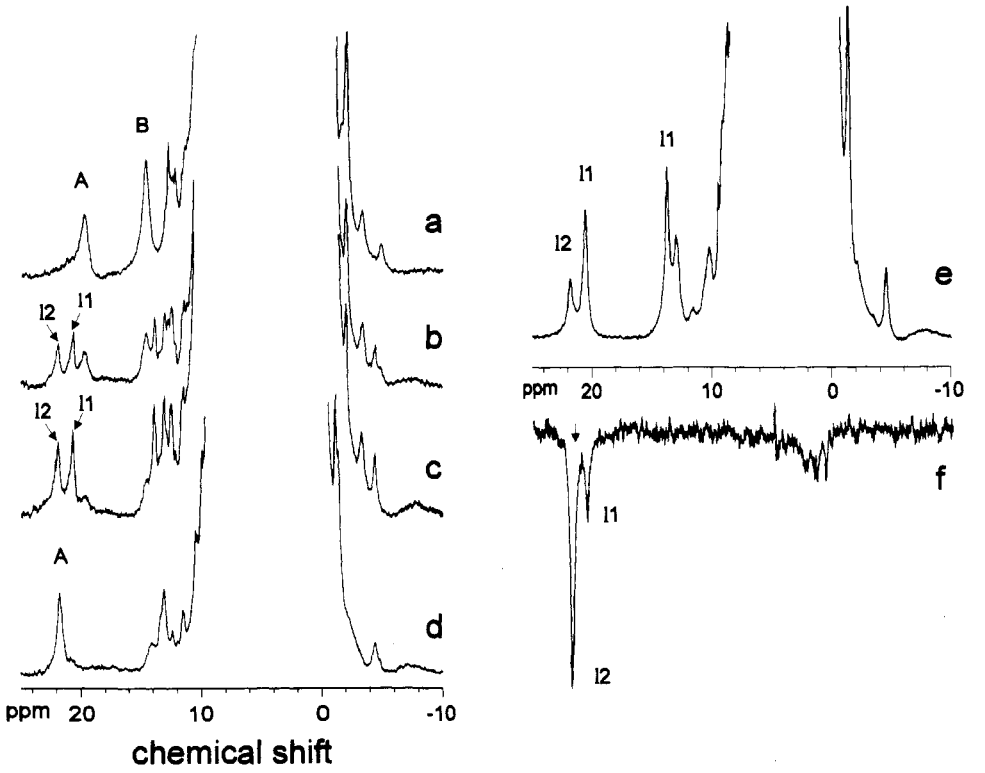

Figure 5. 600-MHz ^{1}H NMR titration of P450 with imidazole, recorded at 600 MHz and 295 K. The titration sample was 0.5 mM in 50 mM Tris–HCl and 50 mM KCl (pH 7.4) in H_2O: (a) P450; (b) P450 + 1 equiv of imidazole; (c) P450 + 2 equiv of imidazole; (d) final imidazole adduct of P450, obtained in the presence of a solution of 0.15 M imidazole. Spectrum e is the reference spectrum and spectrum f is the saturation-transfer difference spectrum obtained upon irradiation of signal A of the I2 species. The arrow in f indicates the irradiated signal. The sample was in 50 mM phosphate buffer (pH 7.1), 50 mM KCl, and 5 mM imidazole in D_2O solution.

P1 and P2, while the third species is a mixed adduct which contains one imidazole and one pyridine molecule (IP hereafter).

Saturation-transfer experiments on the system containing these five different species are quite useful for understanding the nature of the various species. Saturation of the CH_3 signal at 20.5 ppm of the I1 species, again performed with care as described under Materials and Methods, clearly shows saturation-transfer effects on the corresponding signals of I2 and of IP, while no effect is observed on the signals of P1 and P2 (Figure 6). This means that the rate of exchange between I1 and I2 and IP is faster than the nuclear relaxation times of the irradiated signal in the various species, while the rate of exchange is much slower between I1 and both P1 and P2. We propose that I1 contains an imidazole molecule bound to the metal ion, while the second equivalent in I2 is in the hydrophobic pocket.

The aromatic ligand in the hydrophobic pocket is in faster exchange with the free one than that bound to the iron ion. Consequently, saturation transfer from the adduct with imidazole to the iron ion (I1) can be observed only with those species which have a ligand in the hydrophobic pocket (I2 and IP). This means that IP has the imidazole molecule bound to the metal ion, while the pyridine molecule is bound in the hydrophobic pocket.

Hints for the Assignment of the ^{1}H NMR Spectra of the Aromatic Base Adducts of P450. Since we now understand the chemistry of the interaction of aromatic bases with P450, we can take advantage of the relatively good quality of the spectra of these low-spin adducts. The NMR spectra of the inhibitor derivatives show relatively sharp signals (line widths of 200–360 Hz) with similar shift values. Two downfield-shifted signals of intensity 3 are present in all the spectra, other composite signals also being present.

The temperature dependence of the shift values for the hyperfine shifted signals of the three adducts is reported in Figure 7. It can be seen that all the signals show a Curie-type behavior. All the signals have an intercept at the infinite-temperature limit,

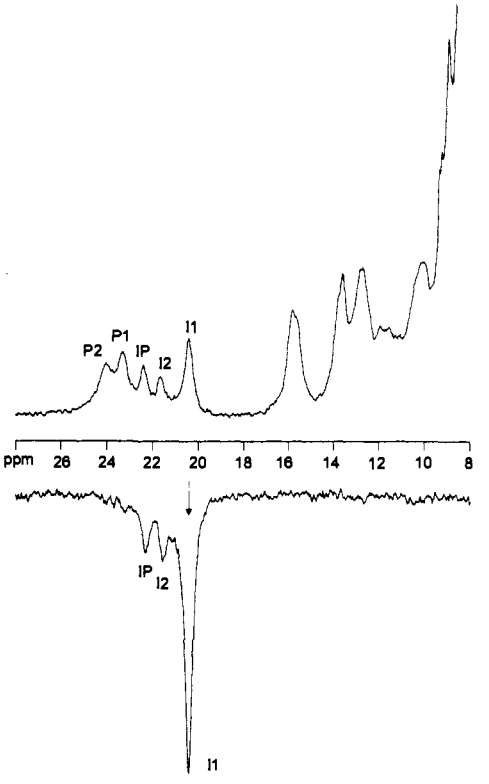

Figure 6. Saturation-transfer experiment performed on signal A of the I1 species. The arrow indicates the irradiated signal. The sample was in 50 mM phosphate buffer (pH 7.1), 50 mM KCl, and 5 mM imidazole in the presence of pyridine in D_2O solution.

essentially to diamagnetic shift values, except a signal around 12 ppm for the pyridine adduct which extrapolates to a negative shift value (−12 ppm). The T_1 values and the line widths of the

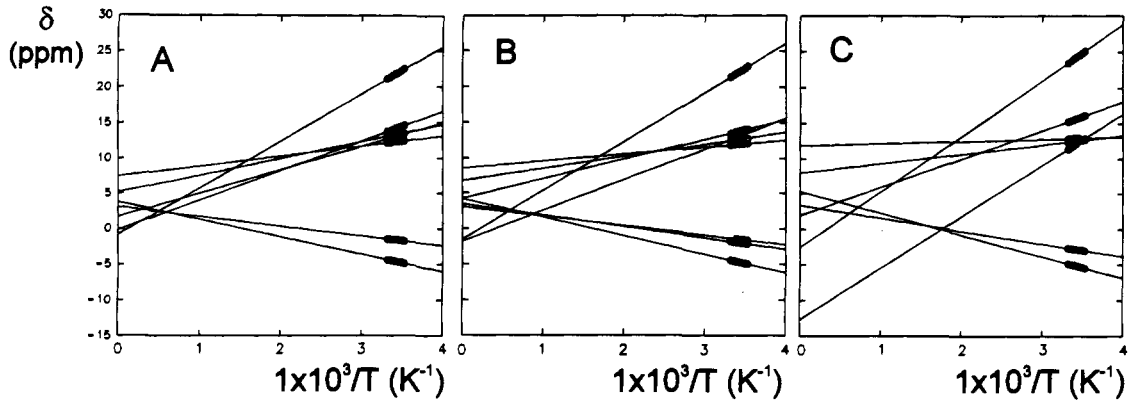

Figure 7. Temperature dependence of the shift values for the paramagnetically shifted signals of the adducts of P450 with (A) imidazole, (B) *N*-methylimidazole, and (C) pyridine.

Table 2. T_1 and Line Width Values for the Two Methyl Signals in the Low-Spin Adducts of P450 Studied in This Work

	final adduct				first adduct			
	signal A		signal B		signal A		signal B	
derivative	T_1,[a] ms	$\Delta\nu$, Hz	T_1,[a] ms	$\Delta\nu$ Hz	T_1,[a] ms	$\Delta\nu$, Hz	T_1,[a] ms	$\Delta\nu$, Hz
substrate free	*b*	500	*b*	430				
imidazole	7.5	350	*c*	*c*	7.0	250	7.7	220
N-methylimidazole	8.2	300	*c*	*c*	7.8	230	8.4	200
pyridine	5.1	360	5.8	250		300		250

[a] T_1 values were measured with an error of ±10%. [b] Not determined, as P450 without substrate is unstable. [c] Not determined, as the signal is within a complex envelope.

paramagnetically shifted signals are reported in Table 2. They are measured as nonselective T_1's.[48] It has already been shown by us[49] that, for short T_1 values such as those reported in Table 2, the difference between selective and nonselective T_1's is below 10% and that the magnetization decay is nonexponential.

The shift values are less well-spread than those for other heme-containing low-spin systems.[31] This makes the application of high-resolution NMR techniques more difficult. We have chosen the pyridine adduct for a further characterization due to the relatively high spectral resolution.

The NOE difference spectra obtained upon irradiation of the two downfield-shifted resonances are shown in Figure 8. The reference spectrum is shown in Figure 8a. As we have shown,[48,50] the 1D NOE experiments have better sensitivity and accuracy than the 2D experiments when broad signals are involved. Irradiation of signal A shows a NOE with a broad signal at 11.6 ppm. Its large line width indicates a position close to the paramagnetic center, and the shift value, similar to those of other low-spin heme proteins,[31,47] suggests that it could be due to an α proton of one of the heme substituents. Other NOEs are observed with signals at 7.5 and 6.3 ppm as well as with signals in the range 5–0 ppm. Irradiation of signal B gives rise to two very intense NOEs at 1.5 and 0.6 ppm, in addition to some smaller effects on signals in the range 7–1 ppm.

2D NOESY experiments can be helpful in the assignment of the paramagnetic shifts. The downfield section of the map collected at 301 K is reported in Figure 9. Several cross peaks between paramagnetic signals and signals in the diamagnetic region are observed; they have been confirmed by recording the map also at 295 K.

Signal A clearly shows cross peaks 2–4 with signals at 1.9, 1.3, and 0.5 ppm. The connectivity with the signal at 11.6 ppm,

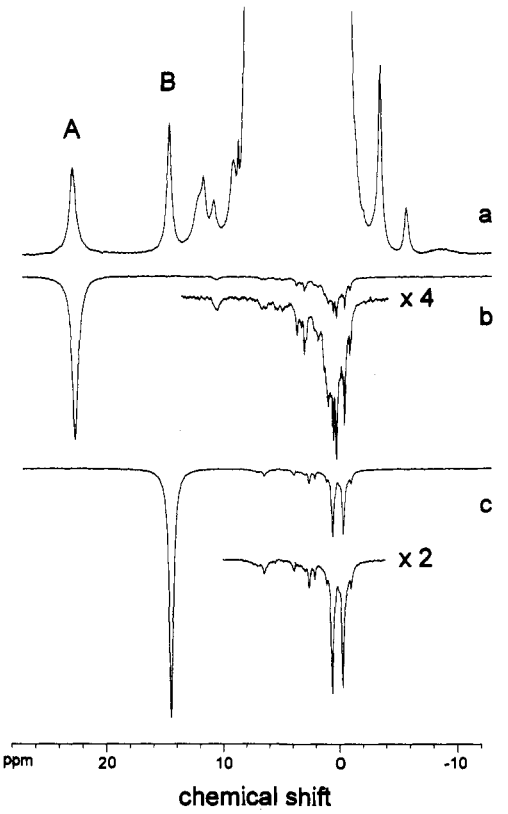

Figure 8. 600-MHz ^{1}H NOE difference spectra of P450 with pyridine. The sample was in 50 mM phosphate buffer (pH 7.1), 50 mM KCl, and 4 mM pyridine in D_2O solution: (a) reference spectrum; (b, c) difference spectra obtained upon irradiation of signals A and B, respectively.

observed in the NOE experiments, is very weak, due to the large line width of the latter signal but is observed in the row passing through signal A. The signal at 11.6 ppm shows a cross peak (5) with a broad signal at 5.9 ppm and a cross peak (6) with the signal at 1.9 ppm, which is also coupled with signal A (2). This pattern of connectivities and of shift values suggests that (a) signal A is due to a CH_3 group close to a propionate chain, (b) the signal at 11.6 ppm is for the α proton of the latter group closer to the CH_3 group, the signal at 5.9 ppm being for the other α proton (the shifts of these α protons are similar to those observed for low-spin peroxidases[31]), and (c) the signal at 1.9 ppm is for the β proton of the same moiety. The signal of the other β proton of the propionate is expected to fall between 1 and 0 ppm. The possibility of signal A being due to a CH_3 group close to a vinyl moiety is further ruled out by inspection of the X-ray structure using computer graphics. The latter shows that both vinyl groups have their α protons (i.e. the protons close to the metal ion) far from the adjacent CH_3 group.

(48) Banci, L.; Bertini, I.; Luchinat, C. *Nuclear and Electron Relaxation. The Magnetic Nucleus-Unpaired Electron Coupling in Solution*; VCH: Weinheim, Germany, 1991.
(49) Banci, L.; Bertini, I.; Luchinat, C.; Piccioli, M. *FEBS Lett.* **1990**, *272*, 175.
(50) Banci, L. *Biol. Magn. Reson.* **1993**, *12*, 79.

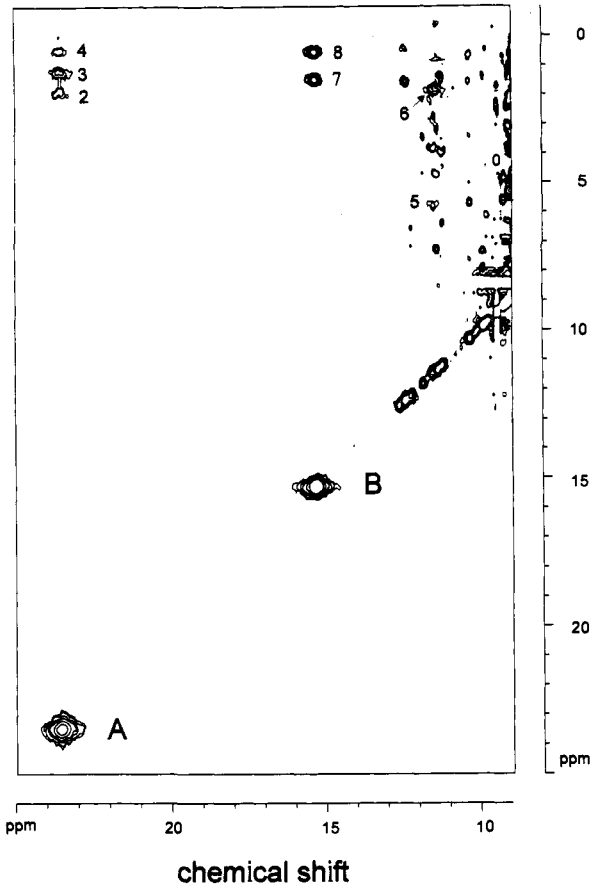

Figure 9. 600-MHz ^{1}H NMR NOESY map recorded with presaturation of the solvent signal during both the relaxation delay (150 ms) and the mixing time (10 ms).

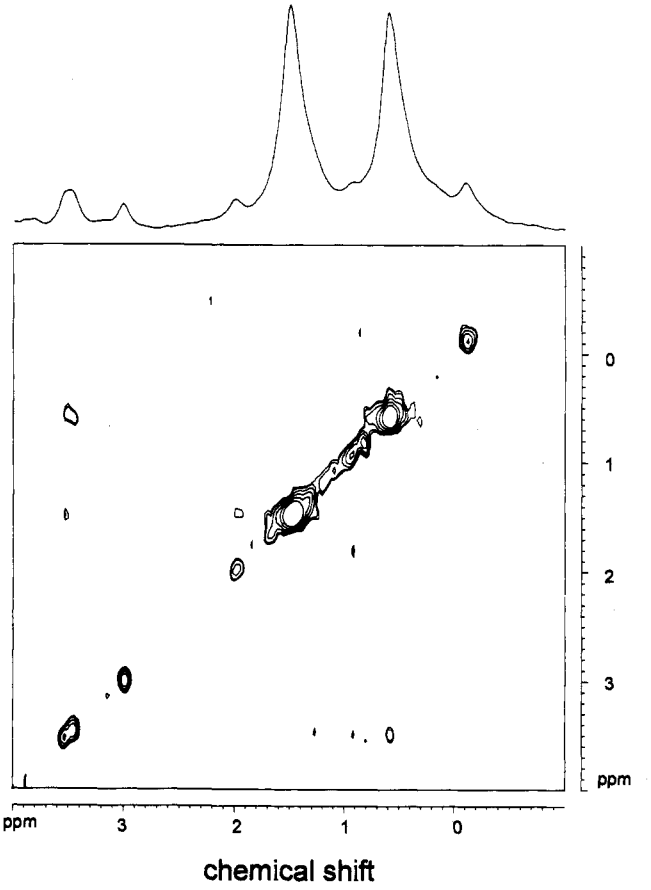

Figure 10. 600-MHz ^{1}H NMR NOE–NOESY spectrum recorded with a mixing time of 20 ms upon selective irradiation of signal B. The difference spectrum obtained upon irradiation of signal B is shown as the reference.

Signal B shows two very intense cross peaks (7 and 8), of similar intensity, with signals at 1.5 and 0.6 ppm. The intensity and the similar magnitude of the two cross peaks suggest that they are not due to protons of the heme substituents. If they were due to β protons of a propionate or of a vinyl group, they would show coupling between each other. We have therefore performed a NOE–NOESY experiment[43] by saturating signal B. In this type of experiment, a difference map is obtained by subtracting from a standard NOESY experiment another NOESY experiment where one signal has been saturated. The map obtained with saturation of signal B is reported in Figure 10, and it shows on the diagonal the signals which are directly coupled with B. Out of the diagonal there are cross peaks between the signals of the latter protons and other protons close to them. We can see clearly that the signals at 1.5 and 0.6 ppm are not dipolarly coupled and therefore they cannot be due to a pair of β protons of a heme substituent. The intensity of the NOE is very large and symmetric. The latter fact indicates that the signals are due to two protons whose signals are at almost the same distance from the methyl B signal. The two signals should also be at a similar distance from the metal ion signal, as in the NOE difference spectrum they show similar line widths. Finally the large intensity of the effect suggests that the two signals could be due to two CH_3 groups. They must be far from each other, as they do not experience any coupling. From inspection of the X-ray structure, we can locate the δ-CH_3 of Leu 362 and the γ-CH_3 of Val 253, which fulfill all the conditions set by the NOE experiments. No pair of single protons can, on the contrary, be in agreement with these conditions. These CH_3 groups are close to the 3-CH_3 of the heme ring. We therefore assign signal B to the 3-CH_3 group. The other resolved CH_3 group is tentatively assigned as 8-CH_3 on the basis of analogy to what occurs in peroxidases and cytochromes. In the former proteins, the plane of the axial histidine makes the four pyrroles pairwise unequivalent, and in the latter class of proteins, the orientation of the S–CH_3 moiety is capable of differencing the pairs 8–3 and 1–5.[31,47] Indeed, the S–CH_2 moiety of the axial cysteine in P450 lies along the line bisecting pyrroles II and IV and therefore makes the d_{xz} and d_{yz} orbitals inequivalent.

In order to learn also about the structure of the other adducts, we have performed NOE experiments on the imidazole and *N*-methylimidazole derivatives, by saturating the two resolved CH_3 signals. The close similarity of observed NOEs for all derivatives indicates that the CH_3 signals have the same shift patterns; i.e., the most downfield-shifted CH_3 is 8-CH_3, while the other resolved group is 3-CH_3.

Saturation Transfer between $P450_{cam}$ and $P450_{py}$. To extend the assignment to the high-spin form of P450, we have attempted saturation transfer between $P450_{cam}$ and the pyridine adduct. The experiments were carried on a sample containing $P450_{cam}$, P1, and P2. The results reported in Figure 11 show a saturation transfer from $P450_{cam}$ to P1 but not to P2, as is clearly evidenced from the saturation transfer from the signal at 40.9 ppm to signal A of P1 (at 23.0 ppm). These experiments have allowed us to recognize the signals of 3-CH_3 and 8-CH_3 in the high-spin species and to recognize the signal of the P1 adduct at –2.5 ppm as a heme methyl signal. The fourth methyl group is most likely hidden around 0 ppm. The detection of saturation transfer from $P450_{cam}$ to P1 and not to P2 indicates that the camphor molecule can exchange relatively fast (rate about 30 s^{-1}) with the species containing a single pyridine molecule.

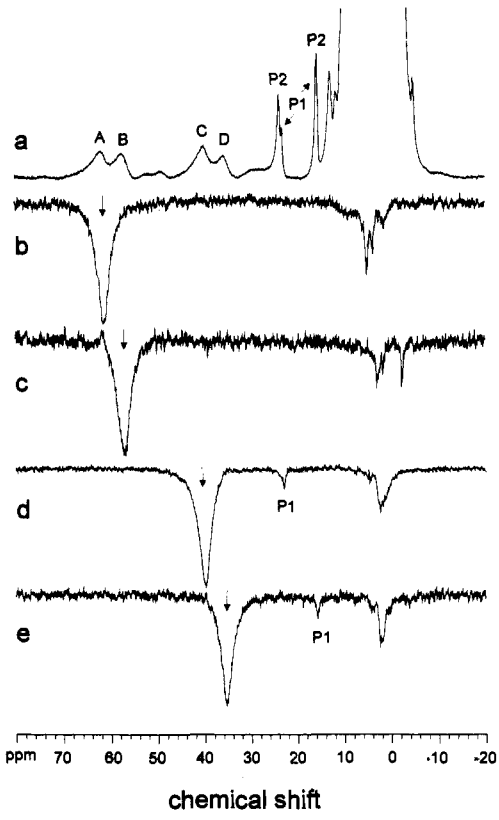

Figure 11. Saturation-transfer experiments performed upon irradiation of signals A–D of $P450_{cam}$ in the presence of pyridine. The arrows indicate the irradiated signals. The protein sample was in 50 mM phosphate buffer (pH 7.1), 50 mM KCl, and 1 mM camphor in the presence of 3 equiv of pyridine in D_2O solution.

Concluding Remarks

The present spectroscopic study on the binding of aromatic bases to P450, both in the presence and in the absence of camphor, has been quite enlightening with respect to the reactivity of the enzyme.

First of all, we have learned that each one of the three bases investigated can bind to P450, by binding to the iron ion and then by interacting with the hydrophobic pocket of the enzyme. The latter property underlines how sizably the hydrophobic interactions are even if they are not selective. As in the case of camphor, van der Waals enthalpic effects as well as entropic effects possibly due to the release of further water molecules from the enzymatic cavity are the factors determining the relatively high affinity for the second equivalent of aromatic bases.[6,15] For the first time, we propose that two ligand molecules can be accommodated in the large cavity of P450. The most convincing evidence is the presence of the ternary complex IP. From this we have learned that both imidazole and pyridine can be simultaneously bound in the cavity, providing a ternary complex, while this does not happen when the camphor molecule is bound in the cavity. The presence of a ternary complex with camphor in the presence of CN^- was suggested.[51]

In the X-ray structure of adducts of phenyl-substituted imidazoles, it has been found that the ligand molecule can be bound either to the iron ion or in the hydrophobic pocket, depending on the steric properties of the ligand.[15]

In the presence of about 1 equiv of pyridine, we have monitored a species containing an aromatic molecule bound to the iron ion which has displaced the solvent molecule. This solvent molecule has been suggested to be the hydroxide ion in P450.[14,15] The H_2O or OH^- nature of the axial ligand is proposed to be essentially determined by the degree of hydrophobicity of the cavity as a result of the number of water molecules still present in the cavity.[14,15]

The *g* values of the adducts with aromatic bases are more anisotropic than those of P450. The T_1 values are shorter and the line widths are broader than those observed in other low-spin heme proteins, such as the cyanide derivatives of globines and peroxidases and low-spin cytochromes. The line widths have similar values at 200 and 600 MHz, indicating that the Curie contributions are smaller. The line widths are essentially determined by the hyperfine dipolar coupling, which is modulated by the electron relaxation time of iron(III). Therefore, it appears that in P450 and its adducts with aromatic bases the electron relaxation times are longer than those in other low-spin iron(III) heme proteins. In their turn, the adducts have shorter electron relaxation times than P450. We may relate electron relaxation times to the extent of the splitting of the d_{xy}, d_{xz}, and d_{yz} orbitals. It appears that low-spin cytochromes and cyanide derivatives of peroxidases and globins have closer orbitals than P450 and P450 with aromatic bases. This can be related to the strength of the metal ion axial ligands: the stronger the axial ligands, the smaller the energy separation between the above d orbitals, the shorter the electron relaxation times, and the larger the *g* anisotropy. All these considerations are again consistent with the proposal that the sixth ligand in P450 is the OH^- group rather than an H_2O molecule.

Finally, the sharper linewidths for the base adducts with respect to P450 have allowed us, through NOE and NOESY experiments, to make for the first time a tentative assignment for the two heme CH_3 signals of other heme substituents and for two other groups around the heme. Saturation-transfer experiments on a mixture of pyridine adduct and $P450_{cam}$ has permitted the assignment of at least two CH_3 groups of the high-spin species and the location of a further CH_3 group in the pyridine adduct.

Acknowledgment. The authors wish to thank Professor Claudio Luchinat for the discussion of the results. S.M. is grateful to the Progetto Finalizzato Chimica Fine II of the CNR for a research fellowship.

(51) Shiro, Y.; Iizuka, T.; Makino, R.; Ishimura, Y.; Morishima, I. *J. Am. Chem. Soc.* **1989**, *111*, 7707.